Original paper

Volcanic history of the Conchagua Peninsula (eastern El Salvador)

Vladislav RAPPRICH[1*], Vojtěch ERBAN[1], Kateřina FÁROVÁ[1], Veronika KOPAČKOVÁ[1], Hervé BELLON[2], Walter HERNÁNDEZ[3]

[1] *Czech Geological Survey, Klárov 3, 118 21 Prague 1, Czech Republic; vladislav.rapprich@geology.cz*
[2] *Université européenne de Bretagne, Université de Bretagne Occidentale, CNRS, UMR 6538 Domaines océaniques, IUEM, 6 av. Le, Gorgeu, CS 93637, 29238 Brest, France*
[3] *Servicio Nacional de Estudios Territoriales (SNET), km 5.5 Calle a Nueva San Salvador, Av. Las Mercedes, San Salvador, El Salvador*
[*] *Corresponding author*

New results of detailed geological mapping, K–Ar dating and geochemical study of the Conchagua Peninsula in eastern El Salvador are presented. Volcanism in the area was controlled by intersection of three tectonic structures, the trench-parallel Central Graben, perpendicular Comayagua Graben, and the Guayape Fault Zone. The age of the volcanic activity spans from Miocene to Quaternary, however, the volcano itself is extinct. The basement is built of the welded rhyolitic Playitas ignimbrite, which extends as far as to the Island of Zacatillo. The pyroclastic rocks of La Unión unit (mean K–Ar age: 13.3 ± 3.7 Ma) display signs of mingling between basaltic and dacitic magmas (banded pumice, deposits containing both mafic scoria and felsic pumice fragments), and this is interpreted as a result of eruptions triggered by injection of a basaltic magma into a dacitic magma chamber. Lavas and pyroclastic flow deposits of the subsequent Pozo unit are poorly exposed and strongly altered. Following effusive activity hereby defined as Pilón Lavas was dominated by andesite and basaltic andesite lavas. Pleistocene volcanic activity is represented by the Pre-Conchagua edifice (1.6 ± 0.6 Ma), Cerro Montoso, El Bable and Juana-Pancha. Regarding the trace-element composition, some lavas of the Pre-Conchagua – Juana-Pancha are distinct from common volcanic front products (lower Zr/Nb, Th/Nb, Ba/Nb), resembling the lavas of Tegucigalpa volcanic field to the north, which is located behind the volcanic arc in the Comayagua Graben. Behind-arc extensional tectonics could have facilitated the magma genesis via decompression melting of the mantle wedge. The current Conchagua Volcano consists of two cones, Ocotal and Banderas, built by repeated Strombolian eruptions associated with effusions of basaltic lavas. The uppermost unit consists of a white tuff preserved in the sedimentary fill of several tectonic valleys west of Conchagua. The white tuff was interpreted as distal fall-out of the Tierra Blanca Joven eruption of the Ilopango Caldera.

Keywords: La Unión, Conchagua Volcano, volcanism, volcanostratigraphy, Central American volcanic chain, Comayagua Graben
Received: 26 March 2010; accepted: 9 July 2010; handling editor: M. Štemprok
The online version of this article (doi: 10.3190/jgeosci.069) contains supplementary electronic material.

1. Introduction

The Conchagua Peninsula is named after the conspicuous Conchagua Volcano, the easternmost promontory of the Salvadorian mainland. Although it is one of the prominent volcanic edifices of the Central American Volcanic Arc (CAVA), its volcanic history is poorly known. The relatively difficult accessibility of this volcano is probably the main reason for a still fragmentary knowledge of its geological history. However, the Conchagua Volcano located on the volcanic chain segment boundary (Carr 1984) provides an opportunity to understand the evolution of this volcanic region by a study of the volcanic stratigraphy, petrology and isotopic dating.

This paper focuses on detailed description of the litho-stratigraphy of the Conchagua Volcano and underlying units, bringing new data and discussion on the tectonic and magmatic evolution of the volcanic arc. Results of detailed geological mapping and analytical work are presented as carried out by the Czech Geological Survey in cooperation with Servicio Nacional de Estudios Territoriales (SNET) in 2003 and 2006. The smaller Salvadorian islands in the Gulf of Fonseca consist of the same volcanic products as the mainland, but the larger islands of Conchagüita and Meanguera (east of Conchagüita) represent independent volcanoes with their own stratigraphy and history, and are beyond the scope of this paper.

2. Geological setting

2.1. Stratigraphy of El Salvador

Six litho-stratigraphic formations were defined for the territory of El Salvador by Wiesemann (1975): (1) Metapán Formation (Jurassic and Cretaceous sediments and volcanic rocks – both mafic and silicic), (2) Morazán Formation (Oligocene volcanic rocks – both mafic and

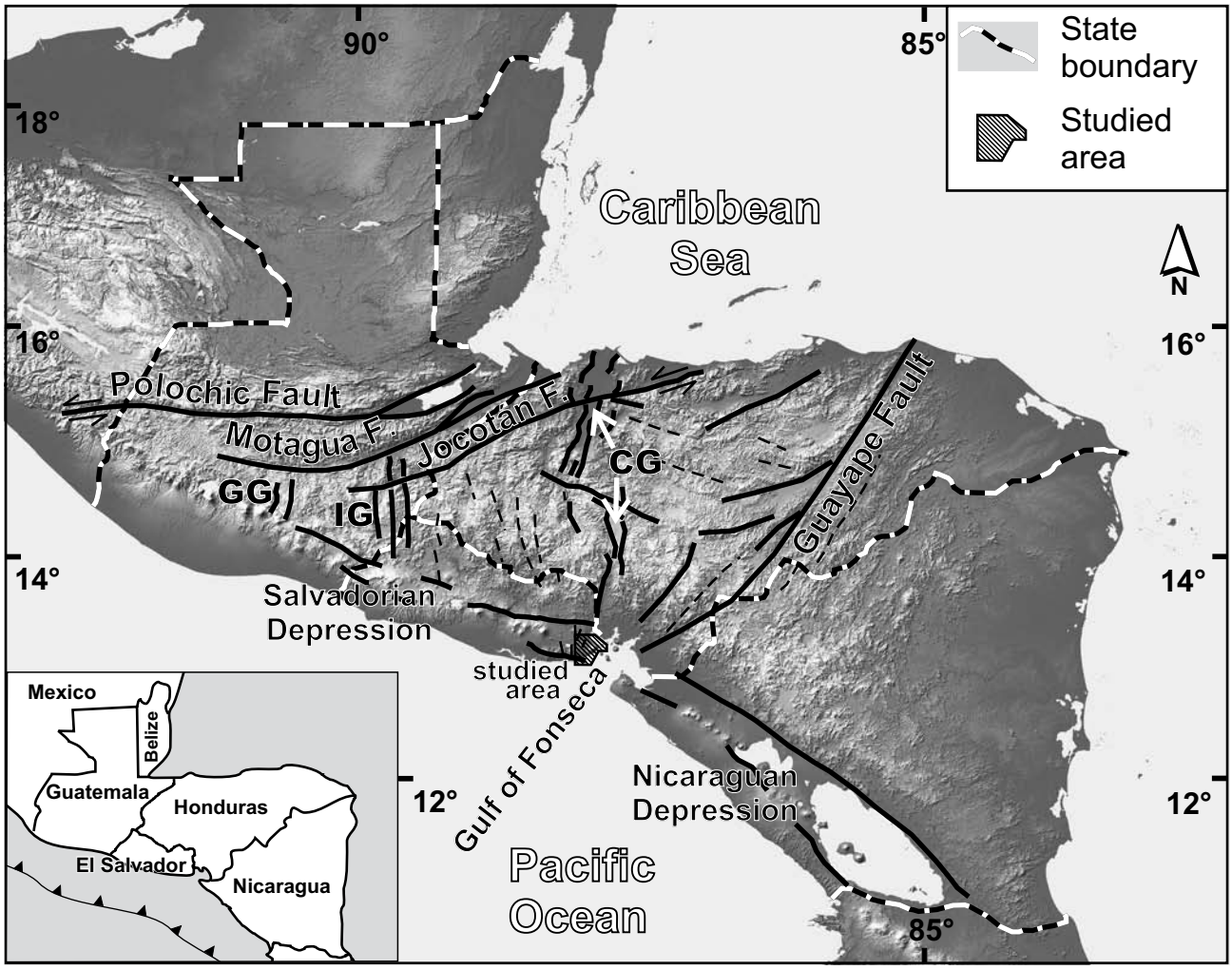

Fig. 1 Digital Elevation Model (DEM) and main tectonic features of the northern Central America: CG – Comayagua Graben (Honduras Depression of Burkart and Self 1985), GG – Guatemala Graben, IG – Ipala Graben. Tectonic setting adapted after Burkart and Self (1985), Finch and Ritchie (1991) and this study. The DEM image of Central America was downloaded from the JPL website, *http://www2.jpl.nasa.gov/srtm/central_america.html.* Scheme with state boundaries and subduction zone is shown in the inset.

silicic), (3) Chalatenango Formation (Miocene volcanic rocks – both mafic and silicic), (4) Bálsamo Formation (Pliocene mafic volcanic rocks), (5) Cuscatlán Formation (Pleistocene volcanic rocks, dominated by silicic lithologies; mafic rocks are subordinate) and (6) San Salvador Formation (Holocene volcanic rocks – both mafic and silicic; fluvial and colluvial sediments). The stratigraphic subdivision is based mainly on superposition of individual units. The geochronological data, with the exception of numerous historically documented eruptions of San Salvador Formation, are scarce.

The Conchagua Volcano, situated south of the town of La Unión and Cutuco seaport, represents the southeasternmost extremity of the Salvadorian part of the Central American Volcanic Arc (Fig. 1). The current edifice consists of two cones: Ocotal (1225 m a.s.l.) and Banderas (1156 m a.s.l.). Weber et al. (1974) mapped in the area only two of the six formations mentioned above. The edifices of Conchagua (including both Ocotal and Banderas), Juana-Pancha and volcaniclastic deposits in the vicinity of La Unión belong to the Cuscatlán Formation. Volcanic rocks between Conchagua and the Olomega Lake (west of studied area) were classified as belonging to the Bálsamo Formation.

2.2. Tectonic setting of the Gulf of Fonseca

The Gulf of Fonseca is located upon intersection of three important tectonic structures (Fig. 1). The Central Graben (*syn.* Salvadorian Depression or Median Trough, called Nicaraguan Depression further to the SE) is parallel to the Middle America Trench and originated in response to extension related to the subduction roll-back of the Cocos Plate (Phipps–Morgan et al. 2008; Funk et al. 2009).

Present-day dextral strike-slip movements on the El Salvador Fault Zone (the northern edge of the Salvadorian Depression) were described by Corti et al. (2005). These dextral movements are interpreted as accommodating the oblique subduction. The Comayagua Graben is thought to have formed as a result of extension related to eastward escape of the Chortis Block (Burkart and Self 1985). The Guayape Fault runs from the Gulf of Fonseca to the northeast (Finch and Ritchie 1991). Silva–Romo (2008) interpreted this fault as a Mesozoic terrane boundary, originally being a part of the Guayape–Papalutla Fault Zone. There is an ongoing debate on the character of this fault zone in several papers published within the last years. Early studies supposed sinistral movement (Burkart and Self 1985). Indeed, sinistral displacement exceeding 50 km was documented by Finch and Ritchie (1991), but these authors have also observed several dextral strike-slip basins evidencing a later dextral movement phase. Dextral motion on the Guayape Fault is probably caused by anticlockwise rotation of the Chortis Block (Gordon and Muehlberger 1994).

2.3. Previous studies of the Conchagua Volcano

Reports on seismic activity around the volcano by Sapper (1925) are the earliest geological data ever published. Boulders released by seismic tremors and rolling down the volcano slopes were repeatedly (e.g., in 1868 and 1892) interpreted as a manifestation of volcanic activity (e.g., Meyer–Abich 1956). These events were often reported as eruptions in many popular volcanic encyclopaedias, although the Global Volcanism Program summary (2009) correctly described all these events (including also 1522, 1688 and 1947) as earthquake-triggered landslides/rock-falls.

Brief field observations were carried out during a German geological expedition in late 1960's, resulting in a synoptic geological map (Weber et al. 1974; Weber and Wiesemann 1978) and regional summaries (Wiesemann 1975; Weyl 1980). An unpublished geological map on the scale 1:50 000 was compiled by a geological expedition of the Czech Geological Survey in cooperation with Servicio Nacional de Estudios Territoriales (Hradecký et al. 2003). The chemical composition of erupted lavas was discussed, in broader regional context, by Carr et al. (1981, 2003); further compositional data were also given by Bolge et al. (2009) and Tonarini et al. (2007).

3. Methods

The present work is principally based on field observations and analytical data acquired within a six-week expedition in 2003 complemented with a second, short field campaign in 2006. All available outcrops were documented during the field work. Several thin sections from each lithological unit were studied to characterize the main rock types. Additionally, representative rock samples were taken for whole-rock chemical analyses.

3.1. Geological mapping and morphometry

The original geological map enclosed in the final report of Hradecký et al. (2003) was updated by new field observations in 2006 and results of a morphometric analyses (Supplementary material). The morphometric analysis began by generating Digital Elevation Model (DEM) from vector contours at 10 m interval (vectorized topographic maps on the scale 1:25 000) and by consequent extraction of the slope component from the DEM. The DEM was further parameterised in ENVI software using the algorithm proposed by Wood (1996). First, the topographic slope was calculated for every pixel and the maximum and minimum convexity values were assigned. The variation of these parameters was quantified with respect to neighbouring pixels (in orthogonal directions), and then, each pixel was assigned to one of six morphometric classes: ridge, channel, plane, peak, pit, or pass. Only three of the six defined classes are taken into account, as the peaks, pits and passes occur scarcely. The constructed model was calibrated by running Wood's algorithm with slope tolerance values varying between 0.3 and 3.5 degrees and convexity tolerance values ranging from 0.001 to 1.000. The resultant morphometric classes were colour-coded and visualized; the best result was achieved by draping the colour-coded morphometric classes over a three-dimensional map formed by the fusion of an altitudinal map using ArcGIS 3D Analyst SW. The best fit occurred with slope tolerance of 3.0 degrees and curvature tolerance of 0.02. A thematic raster was created from the DEM by grouping slope values into six classes: 1 (inclination 0–5°), 2 (5–10°), 3 (10–15°), 4 (15–20°), 5 (20–25°) and 6 (inclination > 25°). In order to classify the morphometric classes (ridge, plane, and channel) with respect to slope gradient, a matrix analysis was applied using SW Edras Imagine 9.1. Matrix analysis produced a new thematic layer (3×6 classes) that contained a separate class for every coincidence of the selected classes in the morphometric map (ridge, channel, plane) and in the thematic slope map as well (slope classes 1–6). As result, a map classifying three morphometric features was constructed (Supplementary material). The morphometric map was applied to establish the lithological limits more precisely (e.g., lava-flow fronts) and to construct the setting of tectonic lineaments. The GEOrient software (Holcombe 2009) was applied for statistic evaluation of fault orientation and visualization of these data.

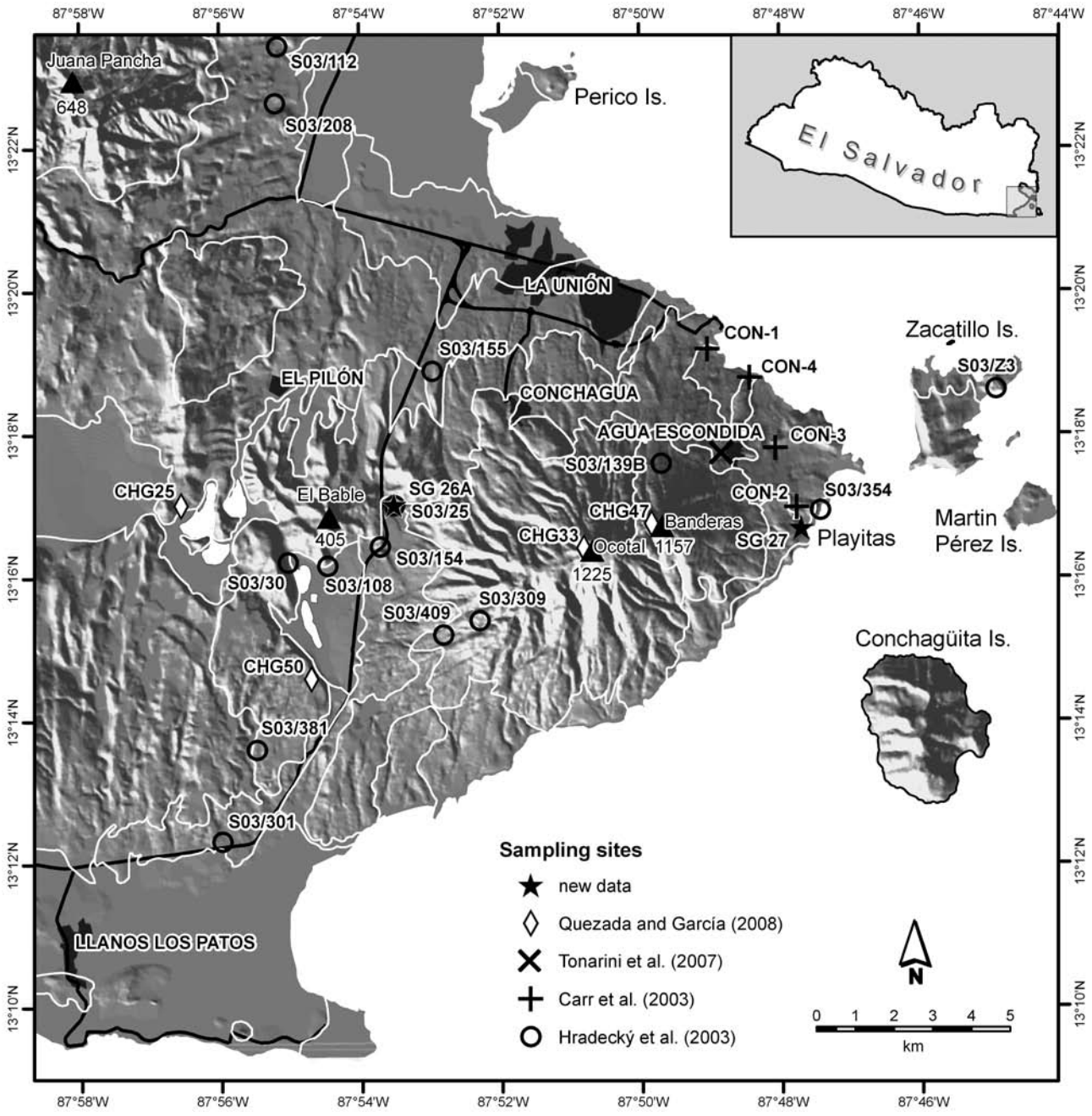

Fig. 2 Digital Elevation Model (DEM) image of the Conchagua Peninsula with Salvadorian islands in the Gulf of Fonseca, principal municipals, roads, peaks and sampling sites indicated. Extent of individual lithological units limited by white lines.

3.2. Whole-rock geochemistry

Fourteen whole-rock samples from the 2003 field campaign (Fig. 2) were analysed by wet chemistry for major-element concentrations in the laboratories of the Czech Geological Survey, Prague. The X-ray fluorescence analyses of trace elements were carried out in the same lab using the XRF machine ARL 9400 ADVANT´XP (Tab. 1). Two additional samples obtained in 2006 were analysed in the Activation Laboratories Ltd. (Ancaster, Canada) by ICP-MS (Tab. 2). These samples were fused with lithium metaborate and tetraborate and subsequently dissolved in 5% nitric acid containing an internal standard. For major oxides and selected trace elements (Sr, Ba and V) the samples were run on ICP-OES Thermo Jarrell-Ash ENVIRO II ICP and for the remaining trace elements using a Perkin Elmer SCIEX ELAN 6000 or 6100 ICP-MS.

The sample SG27 processed for Sr and Nd isotopic ratios was dissolved using a combined HF–HCl–HNO_3

Tab. 1 Major-element oxides and selected trace-element analytical data of representative samples from the Conchagua Peninsula.

Sample	S03/354	Z3	S03/154	S03/25	SG26A	S03/301	S03/112	S03/155	S03/208	S03/139B	S03/30	S03/381	SG27	S03/309	S03/409	S03/108
	Playitas I.		LaUnión u.			Pozo u.	Pilón L.			Pre-Conchagua – Juana Pancha				Ocotal		White T.
Lab	CGS	CGS	CGS	CGS	Act	CGS	CGS	CGS	CGS	CGS	CGS	CGS	Act	CGS	CGS	CGS
Rock	ignimbrite	ignimbrite	scoria	pumice	pumice	ignimbrite	lava	lava	lava	lava	lava	lava	lava	lava	scoria	tuff
TAS	rhyolite	rhyolite	basaltic andesite	dacite	andesite	andesite	basaltic andesite	basaltic andesite	basaltic andesite	basaltic andesite	basaltic andesite	basalt	basalt	basalt	basalt	rhyolite
North	13°16'57"	13°18'37"	13°16'26"	13°17'01"	13°17'01"	13°12'19"	13°23'42"	13°18'53"	13°22'38"	13°17'35"	13°16'13"	13°13'36"	13°16'43"	13°15'24"	13°15'12"	13°16'10"
West	87°47'27"	87°44'55"	87°53'43"	87°53'31"	87°53'31"	87°55'59"	87°55'03"	87°52'58"	87°55'12"	87°49'42"	87°55'02"	87°55'29"	87°47'38"	87°52'18"	87°52'49"	87°54'28"
SiO_2	71.89	65.62	50.73	61.49	59.97	54.23	53.22	52.85	53.17	51.93	52.83	47.79	51.53	49.24	48.74	69.26
TiO_2	0.16	0.25	0.75	0.42	0.46	0.62	1.15	0.77	0.83	0.74	0.73	0.75	0.77	0.80	0.91	0.28
Al_2O_3	14.30	13.41	19.40	16.17	16.50	18.21	16.54	19.77	18.08	19.28	19.93	18.51	18.38	20.77	20.19	15.11
Fe_2O_3	1.79	1.54	6.03	1.92	6.07*	5.66	5.18	4.22	6.71	3.29	4.10	3.09	9.36*	3.00	6.14	1.51
FeO	0.17	1.22	3.66	3.50	–	2.44	4.97	3.94	2.87	5.59	4.38	7.26	–	6.62	3.87	0.57
MnO	0.067	0.114	0.203	0.184	0.188	0.145	0.187	0.174	0.155	0.172	0.165	0.190	0.172	0.177	0.182	0.102
MgO	0.23	0.56	3.58	1.72	1.89	2.59	2.87	2.65	3.53	4.51	3.15	6.81	5.24	3.95	2.99	0.29
CaO	1.76	1.58	9.46	5.45	5.35	6.10	7.85	9.06	8.69	9.42	9.39	11.45	9.48	11.23	9.74	1.46
SrO	0.020	0.021	0.057	0.050	–	0.038	0.039	0.055	0.043	0.051	0.054	0.042	–	0.050	0.048	0.014
BaO	0.150	0.143	0.114	0.091	–	0.096	0.112	0.121	0.058	0.045	0.053	0.103	–	0.033	0.042	0.111
Li_2O	0.002	0.001	0.002	0.003	–	0.002	0.003	0.003	0.002	0.002	0.002	0.001	–	0.001	0.002	0.005
Na_2O	4.42	5.32	2.60	3.54	3.39	2.62	3.35	3.44	3.16	2.89	3.06	2.21	2.88	2.53	2.11	3.37
K_2O	2.99	3.20	0.75	1.25	1.20	1.14	1.87	1.05	1.25	0.77	0.98	0.47	0.97	0.50	0.50	2.47
P_2O_5	0.029	0.051	0.170	0.211	0.230	0.098	0.365	0.209	0.126	0.202	0.167	0.106	0.250	0.125	0.129	0.036
H_2O+	0.93	5.77	1.69	3.44	–	3.81	0.96	0.73	1.05	0.82	0.64	0.61	–	0.57	2.45	4.25
H_2O-	0.56	1.08	0.44	0.68	–	1.65	0.74	0.40	0.46	0.19	0.45	0.27	–	0.19	1.66	0.72
CO_2	<0.01	<0.01	<0.01	0.01	–	0.01	0.01	0.04	0.01	<0.01	0.02	0.01	–	<0.01	<0.01	0.02
F	0.035	0.045	0.041	0.046	–	0.044	0.052	0.040	0.044	0.052	0.040	0.034	–	0.037	0.031	0.042
LOI	–	–	–	–	3.83	–	–	–	–	–	–	–	0.04	–	–	–
Total	99.53	100.01	99.69	100.2	99.09	99.53	99.69	99.52	100.23	99.96	100.16	99.72	99.09	99.83	99.75	99.69
Cr	<2	<2	9	3	< 20	5	17	16	14	25	10	29	50	10	12	<2
Cu	15	16	140	31	29	94	259	146	86	113	203	137	120	186	193	21
Nb	3	4	1	1	2	2	6	2	<1	6	<1	<1	8,2	<1	<1	4
Ni	<2	<2	<2	3	< 1	6	7	4	8	16	7	20	30	3	<2	<2
Rb	56	53	10	29	28	23	48	14	24	11	17	4	18	6	8	57
Sr	217	189	519	458	473	355	353	484	434	481	508	417	483	501	428	159
Y	14	30	23	26	19	24	39	32	29	22	24	19	18,2	19	22	23
Zn	35	68	82	81	73	62	108	84	71	76	83	73	80	77	91	49
Zr	144	173	43	90	91	83	183	65	76	61	58	32	68	38	49	137

–: not analyzed; Lab: CGS – laboratories of the Czech Geological Survey, Prague; Act – Activation Laboratories Ltd., Ancaster, Ontario.

Tab. 2 Additional trace-element (including REE) concentrations (Activation Laboratories Ltd., Ancaster, Ontario), Sr–Nd isotopic ratios and analytical data for K–Ar dating.

Sample	SG26A		SG27
	La Unión unit		Pre-Conchagua
Ba	759		508
Cs	1.1		0.4
Hf	2.4		1.8
Ta	0.2		0.6
Th	1.5		1.2
U	1.0		0.5
V	66		256
La	11.4		12.5
Ce	23.9		23.5
Pr	3.51		3.19
Nd	15.3		13.7
Sm	3.6		3.3
Eu	1.2		1.2
Gd	3.7		3.4
Tb	0.6		0.6
Dy	3.7		3.4
Ho	0.8		0.7
Er	2.3		2.0
Tm	0.36		0.29
Yb	2.3		1.9
Lu	0.36		0.29
$^{87}Sr/^{86}Sr$			0.703936
2S(M)			0.000017
$^{143}Nd/^{144}Nd$			0.513001
2S(M)			0.000011
Lab.Ref.$^{+}$	B 7174-8	B 7187-4	B 7173-6
K_2O (wt.%)	0.17	0.17	1.03
$^{40}Ar_R$ (10^{-7} cm^3 g^{-1})	0.686	0.783	0.536
$^{40}Ar_R$ (%)	11.9	6.7	4.3
Molten weight (g)	0.4352	0.4007	0.8012
^{36}Ar (10^{-9} cm^3 exp)	0.75	1.48	3.21
^{36}Ar (10^{-9} cm^3 g^{-1})*	1.43	3.07	3.85
Age (Ma)**	12.5 ± 3.7	14.24 ± 4.7	1.61 ± 0.6
Mean age (Ma)**	13.4 ± 3.7		

$^{+}$: order of the experiment in the Brest laboratory; *: blank corrections for ^{36}Ar, before the calculation of ^{36}Ar per g of grains; **: error at ± 1σ.

attack. Strontium and neodymium were isolated by ion exchange chromatography techniques using the Sr.spec Eichrom resin, and Nd with TRU.spec with Ln.spec Eichrom resins respectively (see Míková and Denková 2007 for details). Isotopic analyses of and the two elements were performed on Finnigan MAT 262 Thermal Ionization Mass Spectrometer in a dynamic mode using a single and double Re filament assemblies, respectively. The Sr and Nd ratios were corrected for mass fractionation assuming $^{146}Nd/^{144}Nd = 0.7219$ and $^{86}Sr/^{88}Sr = 0.1194$. The precision and external reproducibility are shown by repeated analyses of the La Jolla ($^{143}Nd/^{144}Nd = 0.511852 \pm 14$ (2σ; n = 23)) and NBS 987 ($^{87}Sr/^{86}Sr = 0.710247 \pm 26$ (2σ; n = 25)) isotopic reference materials.

Geochemical data were recalculated and plotted using the GCDkit software (Janoušek et al. 2006).

3.3. K-Ar dating

The bulk-rock sample SG27 (Pre-Conchagua) and amphibole separated from the La Unión pumice (SG26A) were dated by H. Bellon using the K–Ar method in Brest (France). The potassium content in samples was measured by atomic absorption spectrometry after an attack by hydrofluoric acid. Argon was released by heating the samples under vacuum in molybdenum crucible, cleaned on three quartz traps containing hot titanium sponge that gathers the active gases at descending temperatures from 800 °C to ambient one. Further cleaning by Al–Zr SAES getter leads to nearly pure argon extracted from the sample for mass spectrometry analysis. Argon isotopic compositions and concentration of radiogenic ^{40}Ar were measured using a stainless steel mass spectrometer with a 180° geometry. The ^{40}Ar and ^{36}Ar concentrations were measured using the isotope dilution procedure with ^{38}Ar buried as ions in aluminium targets as described in Bellon et al. (1981). Ages have been calculated using the constants of Steiger and Jäger (1977). Errors have been estimated after Mahood and Drake (1982), a well-suited calculation scheme for young geological samples. Analytical data and resulting ages are listed in Tab. 2 and 3. Additional Ar–Ar whole-rock plateau age data from the unpublished report of Quezada and García (2008) were also used. All errors quoted in the present paper are given as 1σ.

4. Results

4.1. Volcanic stratigraphy

The rocks in the area of Conchagua Volcano were divided into seven informal lithological units (Tab. 3). The table also presents rough correlation of these units with the regional lithostratigraphy proposed by Wiesemann (1975).

4.1.1. Playitas Ignimbrites

The oldest geological unit observed within the studied area consists of welded rhyolitic ignimbrites. The base

Tab. 3. Lithostratigraphic scheme for the Conchagua Peninsula, including correlation of proposed units with previously published classifications and available geochronological data.

Conchagua litho-stratigraphy (this paper)	Geochronology (this paper) (Ma)	Geochronology (Quezada and García 2008) (Ma)	Conchagua litho--stratigraphy (Hradecký et al. 2003)	General litho-stratigraphy of El Salvador (Wiesemann 1975)*
White ash – Ilopango eruption 430 AD				San Salvador Fm. (Holocene)
Ocotal and Banderas (CHG33, CHG47)		0.15 ± 0.02, 0.41 ± 0.1	Ocotal and Banderas	Cuscatlán Fm. (Pliocene–Pleistocene)
Pre-Conchagua and Juana-Pancha (SG27, CHG13, CHG15, CHG50)	1.6 ± 0.6	1.3 ± 0.4, 1.27 ± 0.06, 1.48 ± 0.02	Superior Andesites	Cuscatlán Fm. (Pliocene–Pleistocene)
Pilón Lavas (CHG25)		8.4 ± 1.2	Inferior Andesites	Bálsamo Fm. (Upper Miocene–Lower Pliocene)
Pozo unit	too altered to be analyzed		Pozo Sequence	Bálsamo Fm. (Upper Miocene–Lower Pliocene)
La Unión unit (SG26)	12.5 ± 3.7, 14.2 ± 4.7		La Unión Sequence	Chalatenango Fm. (Miocene)
Playitas Ignimbrites			Basal Ignimbrites	Morazán Fm. (Oligocene) or Chalatenango Fm. (Miocene)

* We correlate our lithostratigraphic units with stratigraphic scheme of Wiesemann (1975), even though the map of German expedition is showing different geographic distribution of the stratigraphic units.

of the ignimbrites is not exposed, but the height of cliffs where this unit is exposed exceeds 10 m. We infer that thickness of this unit reaches several tens (or even hundreds) of meters. These rocks crop out along the eastern banks of the Conchagua Peninsula, in the eastern part of Zacatillo Island and in an uplifted tectonic block east of the Conchagua town (Fig. 3). All three occurrences are mutually comparable in composition but differ slightly in texture, probably forming distinct facies of a single ignimbrite body. The ignimbrite east of the Conchagua town is fine-grained without visible larger fiamme or lithic clasts. In thin-section, only glass shards and microcrysts of both quartz and feldspar can be observed. On the other hand, the ignimbrite at Playitas contains fiamme up to 25 cm in length. The pumice fragments within the ignimbrite on Zacatillo Island are non-flattened in contrast to its flow-banded matrix. The matrix of ignimbrite is crystal rich and alkali feldspar dominates among phenocrysts. Pumiceous deposits covering the welded ignimbrite on Zacatillo Island probably represent non-welded upper facies of the ignimbrite rather than a separate unit. All three occurrences were assigned to a single unit and it is suggested to rename them as "Playitas Ignimbrites" instead of "Basal Ignimbrites" used by Hradecký et al. (2003). The attribute "Basal" is too general and could be misleading.

4.1.2. La Unión unit

The pyroclastic rocks, both primary and resedimented, of the La Unión unit crop out in several areas around the Conchagua Volcano. These volcaniclastic deposits are well exposed in the surroundings of La Unión and in quarries and road-cuts of the Littoral highway (CA-2). Excellent temporary outcrops were exposed in 2003–2004 on the western outskirts of the La Unión town during construction of a new city by-pass connecting the Pan-American highway (CA-1) with the Cutuco seaport (2.5 km east of La Unión). There are two types of deposits related to the La Unión unit in the studied area. West of the Conchagua Volcano, pyroclastic rocks consisting of mixed pumice/scoriaceous material dominate. To the north and northwest, re-deposited pyroclastic deposits predominate.

In a gravel-pit in the valley between El Bable and Ocotal volcanoes (sampling points SG 26A and S03/25 in Fig. 2), deposits of La Unión unit are characterized by a mixture of basaltic scoriae and dacitic pumice. It is possible to distinguish four units exposed on the face of the gravel-pit (Fig. 4). The products of individual eruptive periods were labelled LU1 to LU4. The base of the LU1 unit does not crop out, but the uppermost 0.6 m of the exposed strata consist of clast-supported mafic scoriae with intercalations of pale-greyish pumice and fine ash. Roughly a one meter-thick base surge deposit of angular fine-lapilli and ash overlies the LU1. The LU2 member is 5 m-thick and consists of both pumice and scoriae. The material is clast-supported with grain-size varying from 1 to 15 cm (with a mode of 2–3 cm). Banded pumices with bands of mafic and felsic composition are especially frequent among the larger clasts. The LU2 member is subdivided into three layers according to the variations in pumice/scoriae ratio. The lower sub-unit is dominated by pumice fragments and includes a 15 cm-thick layer

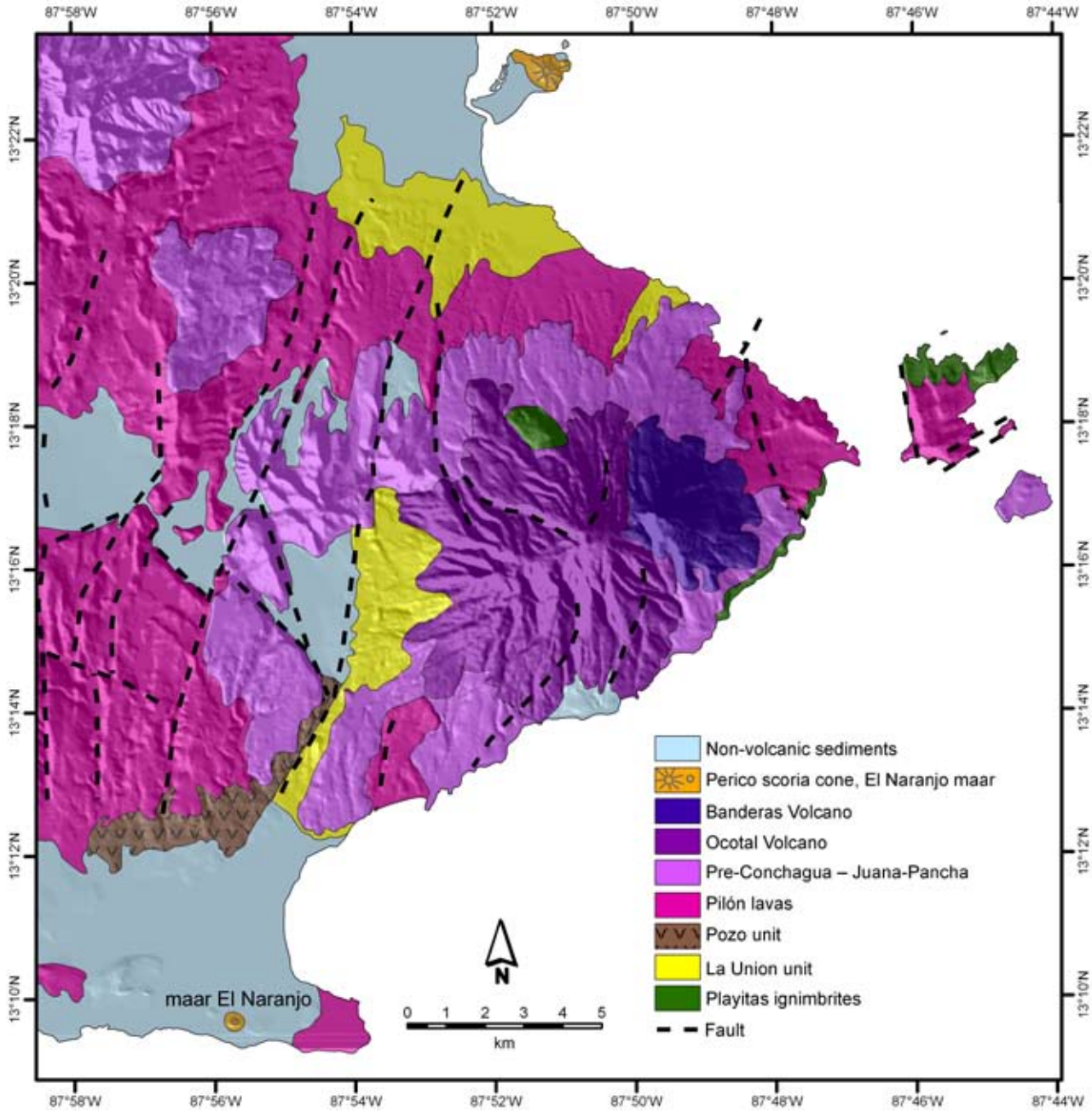

Fig. 3 Simplified geological map of the Conchagua Peninsula (adapted after Hradecký et al. 2003).

of pure black scoriae (Fig. 4). The black scoria layer represents the most mafic product of the La Unión unit. The analysed sample (S03/154) was collected 1 km south, in the same stratigraphic position. The scoria fragments from this sample contain phenocrysts of clinopyroxene (up to 5 mm), plagioclase (up to 2 mm) and pseudomorphs after olivine *c.* 1 mm across. The pumice fragments from the lower sub-unit (sample SG26A) contain abundant phenocrysts of amphibole (up to 2 mm) and alkali feldspar blended with surrounding dacitic glass. The middle sub-unit is dominated by scoria fragments mixed with *c.* 30 % of light-grey pumice, whereas the upper sub-unit is again principally composed of pumice. The LU2 unit is overlain by base surge deposits and a few centimetres-thick pinkish layer of accretionary lapilli not exceeding 1 cm in diameter. The sequence continues with the LU3 unit displaying variable scoria/pumice proportions and a lithics-dominated top followed by a fine tuff layer. The uppermost LU4 unit consists of clast-supported fall-out dominated by dense, non-vesiculated fragments of mafic rock and large scoria fragments (5–10 m). Volcaniclastic deposits of the Ocotal Volcano cover the

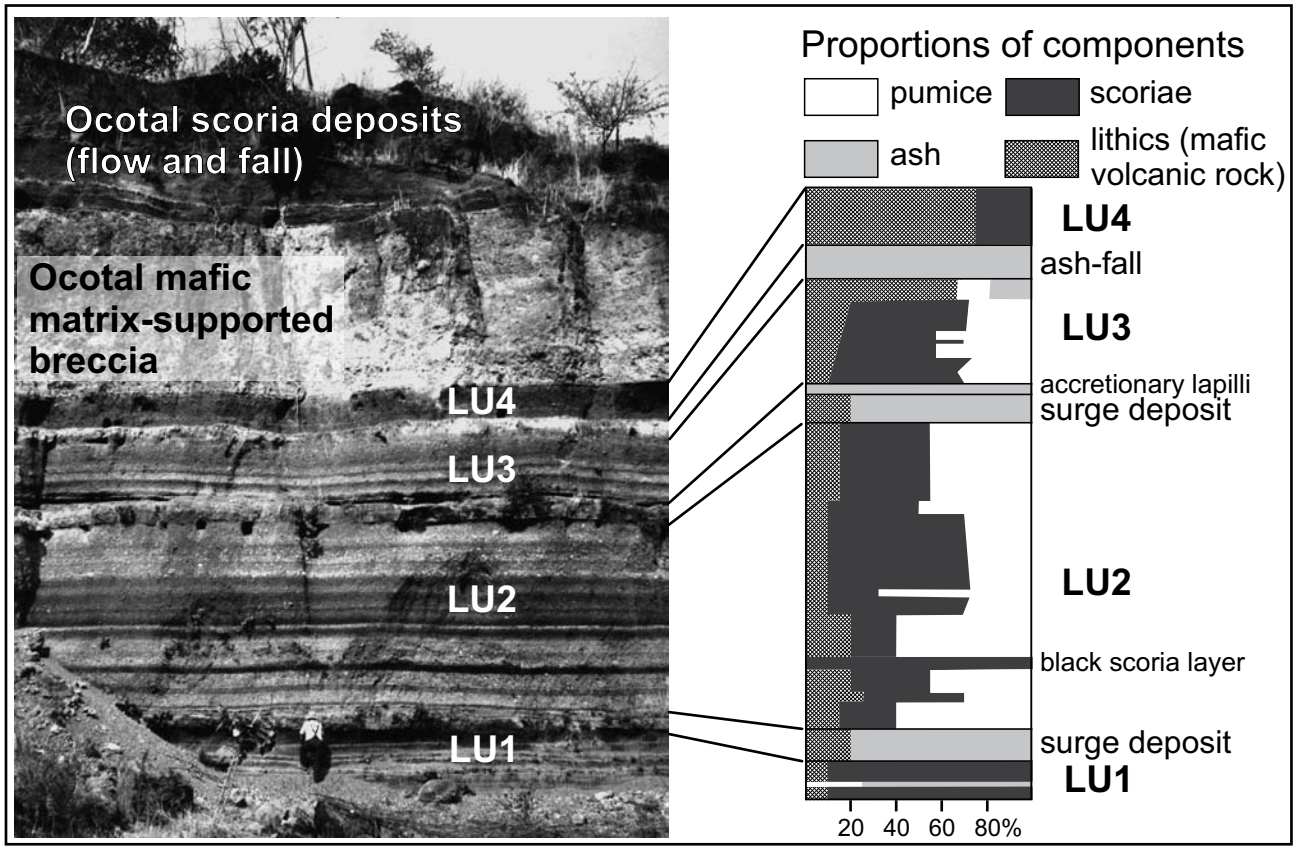

Fig. 4 Sequence of pyroclastic fall-out deposits of the La Unión unit with a evidence of mingling between dissimilar magmas. Note the discordant basal strata of the Ocotal Volcano deposits in the upper part of the image (not shown in the scheme)

entire pyroclastic sequence of La Unión unit on this site. Different facies of the La Unión unit are exposed in the surroundings of La Unión town. Pale-ochre sediments with pumice fragments are cut by channels filled with reworked pumiceous and scoriaceous material (Fig. 5). These deposits are interpreted as mudflows. The fluvial and mudflow deposits alternate several times.

No silica-rich rock was observed above LU4 and the composition of younger volcanic rocks is typically mafic.

4.1.3. Pozo unit

A sequence of strongly weathered andesitic lavas and associated coarse-grained volcaniclastic deposits are found in few outcrops and excavated wells (*pozo* in Spanish) in the southwest part of the study area. Pilón lavas and Pre-Conchagua (or its equivalents) volcanic rocks overlie the Pozo unit, but the base of the Pozo unit is not exposed and the contact with La Unión unit runs along the axis of a narrow and straight NE–SW trending valley south of El Bable. This valley is very probably of tectonic origin. However the exact position of conduits responsible for the production of these volcanic rocks

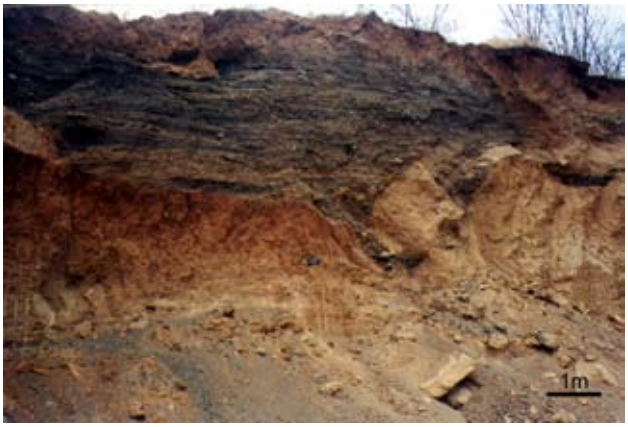

Fig. 5 Re-worked pyroclastic deposits of the La Unión unit. Stream channel cuts into the deposits of pale-ochre mudflows. The channel is filled with cross-bedded scoriae and pumice-lapilli. The cliff is about 6 m high.

remains unclear. Most probably, eroded volcanoes around the Olomega Lake (*c*. 20 km WNW of the Conchagua Volcano) would be good candidates. Unfortunately, these ancient volcanoes have not been studied in detail yet. The analysed sample from this sequence (S03/301) consists of fragments of andesitic rocks, both massive and

vesiculated. The fine-grained matrix seems to be of the same composition as the lithics with crystals of (in order of decreasing abundance) plagioclase, clinopyroxene, amphibole, biotite and Fe-oxides.

4.1.4. Pilón Lavas

Extensive lava sheets of the Pilón Lavas cover large areas between the Olomega Lake and the Gulf of Fonseca. This unit was described as "Inferior Andesites" in Hradecký et al. (2003) but – similarly to the Playitas ignimbrites – a more specific name is preferred here. The lavas consist of typically strongly weathered porphyritic andesites. The Pilón Lavas originally created relatively flat relief, later disrupted by tectonics and erosion. Hence, the effusive centres are difficult to find. Up to 3 m thick layer of weathering products with palaeosoil separates the Pilón Lavas from the overlying Pre-Conchagua, Ocotal or Banderas lavas. North of the studied area, rocks of the San Alejo volcanic complex are interstratified between the Pilón Lavas and the Pre-Conchagua unit (Hradecký et al. 2003).

The Pilón Lavas (samples S03/112, S03/155 and S03/208) are porphyritic with the matrix of plagioclase, pyroxene and magnetite. The most prominent phenocryst phase is plagioclase reaching 4 mm. Pyroxene, olivine and magnetite phenocrysts usually do not exceed 1 mm, except for clinopyroxene in S03/208, where it may reach 4 mm. A rock sample corresponding to the Pilón Lavas was dated by Quezada and García (2008) to 8.4 ± 1.2 Ma (Ar–Ar plateau age).

4.1.5. Pre-Conchagua – Juana-Pancha

The morphology of this younger sequence of lavas is better preserved. The unit comprises lava flows from four volcanoes in the studied area: Pre-Conchagua, Juana-Pancha, Cerro Montoso and El Bable (Figs 2 and 3). Pre-Conchagua lavas build the lower part of the Conchagua Volcano beneath the current Ocotal and Banderas cones. On several places within the El Bable Volcano, intercalations of scoriae deposits and lava flows were interpreted as products of Strombolian eruptions. Quezada and García (2008) presented Ar–Ar (plateau age) data for one lava flow south of El Bable (1.3 ± 0.4 Ma) and for two samples from the western slope of the Juana-Pancha Volcano (1.27 ± 0.06 and 1.48 ± 0.02 Ma). The general alignment of the four volcanoes belonging to this formation (Pre-Conchagua, Juana-Pancha, Cerro Montoso and El Bable) is from north–northwest to south–southeast (oblique to the current volcanic front). The eastern limit of the lava flows is marked by an occurrence of pillow breccia on the eastern side of the Martin Peréz Island (Fig. 6). The breccia consists of pillows, cauliflower

Fig. 6 Pillow breccia of andesitic lava in the Pre-Conchagua – Juana-Pancha unit, on the eastern bank of the Martin Pérez Island.

and irregular fragments of the lava quenched upon their contact with water. The fragments are mantled with argillitized palagonite and enclosed in a reddish matrix of argillitized glass. Poorly-sorted sedimentary breccia interpreted as debris flow deposits crops out on the northern and southern shores of the Conchagua Peninsula. The fragments are up to 50 cm in diameter, consist of well-crystallized basaltic andesite lava and are enclosed in a pale brownish clayey to sandy matrix. The large volume of these debris flow deposits suggests a significant phase of the volcanic edifice decay.

Basaltic lava from the Pre-Conchagua Volcano sampled at Playitas (sample SG27) contains phenocrysts of clinopyroxene, olivine and plagioclase (anorthite to labradorite) in a matrix of clinopyroxene, orthopyroxene, olivine, plagioclase and Fe–Ti oxides. The other samples (S03/139B, S03/30 and S03/381) vary in composition between basalt and basaltic andesite and are very similar in petrography. The rocks are porphyritic with matrix of plagioclase, pyroxene and magnetite. The proportions of phenocryst phases are slightly variable. Plagioclase (up to 6 mm) is the most abundant phenocryst phase in all three samples. In the sample S03/139B, olivine forms abundant phenocrysts (up to 3 mm), which may merge to glomerocrysts. Clinopyroxene phenocrysts are similar to olivine in size, but occur less frequently. Sample S03/30 is relatively rich in olivine (about 1 mm), but clinopyroxene is scarce. On the other hand, clinopyroxene is more frequent than olivine in the sample S03/381.

4.1.6. Ocotal and Banderas volcanoes

The Ocotal and Banderas summit cones form the present-day Conchagua Volcano. Ocotal cone is symmetric and regular, in contrast to the asymmetric Banderas cone. The Banderas asymmetry is mainly due to its horseshoe shaped crater oriented to the northeast. The Banderas cone is much less affected by faults and its lavas are less

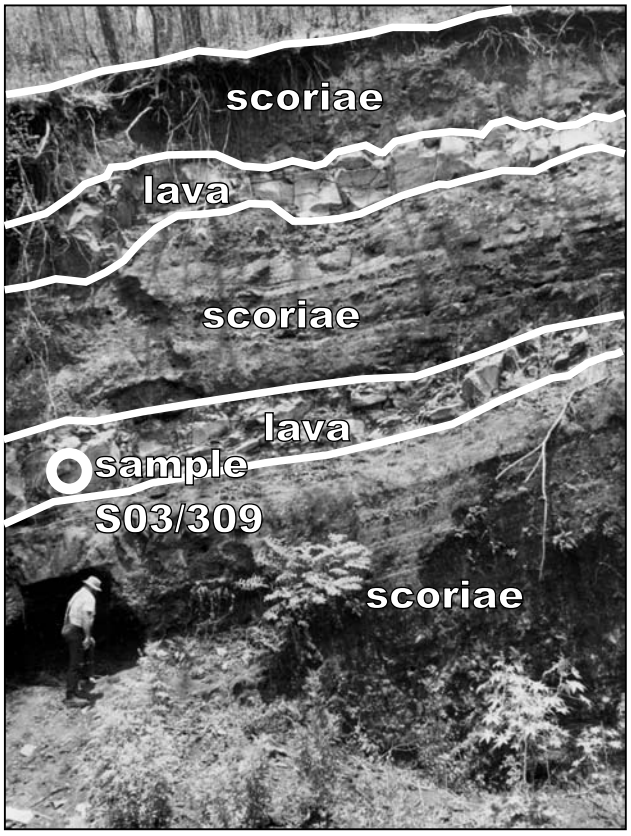

Fig. 7 Profile in scoriaceous deposits alternating with basaltic lavas exposed in a quarry in the western flank of the Ocotal cone.

weathered. A younger age for Banderas was estimated by Weber and Wiesemann (1978); Hradecký et al. (2003) suggested the opposite, but no supporting arguments were provided. The Ar–Ar data by Quezada and García (2008) indeed show a younger age for Ocotal (0.15 ± 0.02 Ma) and an older age for Banderas (0.41 ± 0.1 Ma).

Mafic matrix-supported breccia with a layer of low-angle planar cross-bedded tuff at the bottom were observed at the base of the volcanic rocks of the Ocotal Volcano (Fig. 4). The matrix dominates the deposit and encloses lithics of mafic volcanic rock (basaltic andesite) up to 20 cm in diameter. The lithics are massive, poorly vesiculated.

The breccia is overlain by scoriae with intercalation of lavas building up the edifice of the Ocotal cone. The scoriae are clast-supported, sorted, layered and non-welded. Individual layers and outcrops differ in grading and angle of dipping strata according to the depositional distance and the nature of sedimentation processes on the volcano slopes (fall, grain-flow, etc.). Scoria fragments of several centimetres predominate in the deposits suggesting low fragmentation index. The thickness of lava flows never exceeds 1 m and these are subordinate compared to scoriae (Fig. 7). The divides between coherent lava and clastic facies are sharp and straight. Lavas have no breccias at the base and only minor autoclastic breccias at the top. The basalt is irregularly jointed, as columnar jointing could not probably form due to low thickness of the lava. There was no fossil soil or fossil weathering observed in the profile.

Deposits of the adjacent Banderas cone are very similar, dominated by non-welded, sorted layered and clast-supported scoriae with intercalations of lavas. The basaltic lavas are spread at the foothill of the volcano. The pyroclastic rocks of the Banderas seem to partly overlay the rocks of the Ocotal, but significant layers of soil cover both cones. We did not observe fresh volcanic material that may suggest historic activity on the Banderas cone.

The studied basaltic lava of the Ocotal Volcano (sample S03/309) consists of olivine and plagioclase (bytownite to labradorite) phenocrysts in matrix of plagioclase (sodic labradorite to andesine), clinopyroxene, olivine and Fe–Ti oxides.

4.1.7. Monogenic cones of uncertain age

Remnants of two monogenic volcanoes crop out in the studied area. The northern part of the Perico Island consists of basaltic cinder cone rimmed by non-volcanic sediments with oyster-shell bank deposits. Deposits of this scoria cone are intensively weathered and the cone may correspond temporally to the Ocotal or Banderas volcanoes.

El Naranjo maar east of Llanos los Patos (Fig. 3) is represented by a tuff-ring remnant. The tuff-ring consists of base-surge and unsorted near-vent pyroclastic fall-out deposits of a phreatomagmatic eruption. Hradecký et al. (2003) described palaeobotanical material collected from the phreatomagmatic pyroclastics that included pine needles. The pine-trees currently grow at higher altitudes but not near the modern shoreline in El Salvador.

4.1.8. White ash

The youngest volcanic deposit observed in the studied area is a fine white ash, deposited in shallow lakes and marshes within the tectonic depressions surrounding the El Bable Volcano (see plains with lakes in white on Fig. 2). The white ash is covered with 0.5–1 m of black humic-soil. The complete profile of this ash is exposed in a pit south of El Bable (sample S03/108). Six normal graded sedimentary cycles built up the total thickness of 1.5 m. The grading is characterized by a transition from fine sand to clay grain-size. The base of each cycle is marked by secondary ochre pigment of Fe oxides/hydroxides. The tuff consists of quartz, feldspar and shards of fresh glass.

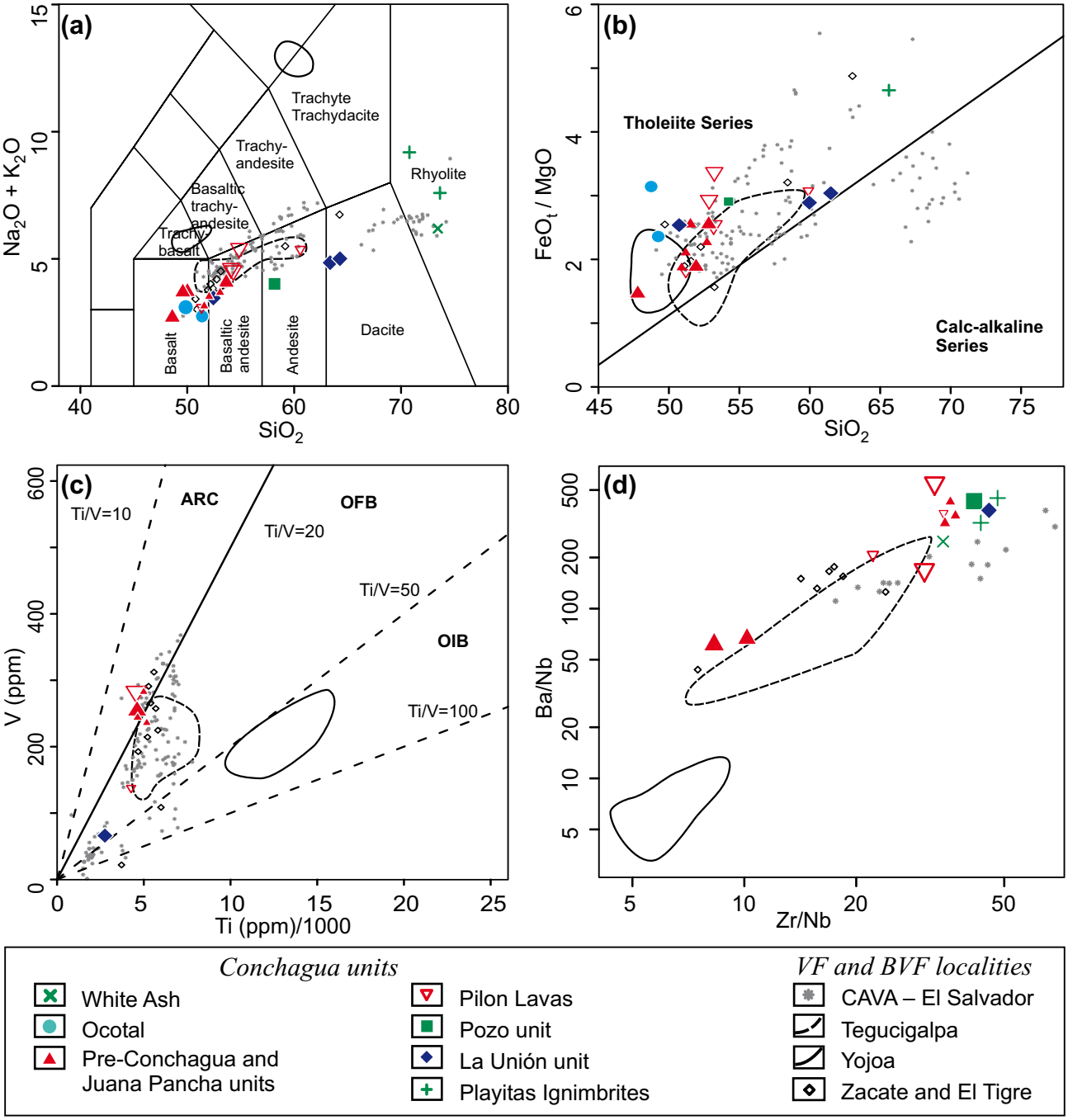

Fig. 8 Selected geochemical diagrams for samples from the Conchagua area. **a** – TAS diagram (Le Bas et al. 1986). **b** – Binary diagram SiO_2 vs. FeO_t/MgO after Miyashiro (1974). **c** – Ti–V diagram, proposed by Shervais (1992) for basaltic lavas. ARC – volcanic arc basalts, OFB – ocean-floor and back-arc basalts, OIB – ocean island and alkaline basalts. **d** – Binary plot Zr/Nb – Ba/Nb, combining subduction component indicator (Ba/Nb) and mantle source enrichment indicator (Zr/Nb). Large symbols were used for new analyses, small for literature data. Analytical data for the volcanic front (VF: CAVA, Central American Volcanic Arc) and behind-volcanic front (BVF: Tegucigalpa, Yojoa, Zacate and El Tigre) lavas in El Salvador and Honduras taken from Carr et al. (2003), Tonarini et al. (2007) and Bolge et al. (2009).

4.2. Geochemistry of erupted magmas

The newly obtained set of major- and trace-element analyses (Tab. 1 and 2) of volcanic rocks from the Conchagua area was supplemented by literature data (CON-1–4 from Carr et al. 2003 and Bolge et al. 2009; ES 48 from Tonarini et al. 2007). The probable lithostratigraphic position of published samples was judged on the basis of

available GPS coordinates (see Figs 2 and 3). Thus the samples CON-1, CON-2 and ES 48 were identified as likely Pre-Conchagua rocks, whereas CON-3 and CON-4 correspond to Pilón Lavas. The available twenty-one chemical analyses represent the lithostratigraphic units described in this paper and provide an overview of the magmatic evolution of the Conchagua Peninsula.

The studied Conchagua volcanic rocks range from basalt to rhyolite, although samples of basic and intermediate composition predominate (Fig. 8a).

The lowermost "Playitas Ignimbrites" unit is represented by two samples of rhyolitic composition (Le Bas et al. 1986). The total H_2O content of the sample Z3 is as high as 5 %, making its original composition questionable. However, in the classification scheme using contents of relatively immobile elements, the samples rank into rhyolite/dacite field (Pearce 1996). Three analyses represent the La Unión unit. Sample S03/154, falling on the boundary between basalt and basaltic andesite, corresponds to the "black scoria layer" in Fig. 4. The other two samples, separated pumice fragments, are of felsic andesite to dacite composition, based on the recalculation on water-free basis. Due to scarce outcrops and intense chemical alteration (possible contribution of weathering and hydrothermal alteration), only one sample of the andesitic ignimbrite from the Pozo unit was analyzed. All samples of the Pilón Lavas and the Pre-Conchagua, Juana-Pancha and El Bable volcanoes range between basalts and basaltic andesites; the two analyses from the Ocotal flanks are exclusively basaltic.

The MgO content in all samples is less than 7 wt. %; low contents of mantle-compatible elements, even for the least evolved samples (Ni < 20.3 ppm, Cr < 30 ppm), are also typical.

The steep trends in the SiO_2 vs. FeO_t/MgO diagram for the Pilón Lavas and Pre-Conchagua – Juana-Pancha, as well as one Pozo and two Ocotal Volcano samples, point towards the tholeiitic series. On the other hand, the flat trend of three La Unión samples implies a calc-alkaline affinity (Fig. 8b).

Except for samples SG27 and SG26A, the Ba content was determined as oxide, and thus the precision is lower. Especially Ba contents in samples S03/S381, S03/154, S03/155 and S03/301 seem overestimated, considering their unusually high Ba/La ratio (up to 280) or high Ba content at given MgO contents. Few lavas in the database of Carr (2003) have Ba/La over 130 and none over 150. The complete trace-element data (see Tab. 2) were only obtained for samples SG27 and SG26A of the new data set.

High-field strength elements contents are generally low. Apart from rhyolites, all studied rocks (except the Pilón Lavas sample S03/112) are low in TiO_2 (<1.0 wt. %), as well as Nb (<10 ppm) and Zr (<100 ppm). Large ion lithophile elements (LILE) are generally high (e.g., Ba 295–1083 ppm, Rb 4–48 ppm). The Ti/V ratios for samples SG27 and SG26A, together with literature data from the Conchagua area, reach ~ 16–31 (Fig. 8c). The value of Zr/Nb ratio is generally above 30, but S03/139B and SG27 (Pre-Conchagua – Juana-Pancha unit) attain only 10.2 and 8.3, respectively. Similarly, Ba/Nb for these two samples is 67 and 62, while for all other Conchagua samples the ratio is higher than 167 (Fig. 8d). Similarly anomalous in comparison with other CAVA lavas in El Salvador (Carr et al. 2003) appears the sample SG27 in geochemical indices involving REE and Th, such as relatively low Ba/La (40) and Th/Nb (0.14), elevated La/Yb (6.7), La/Sm (3.8), or Nb/Yb (4.4).

All five available Sr–Nd analyses, that for the sample SG27 (Tab. 2) and literature data given by Bolge (2005) and Tonarini et al. (2007), cluster within a relatively narrow field around 0.7039 for $^{87}Sr/^{86}Sr$ and slightly above 0.5130 for $^{143}Nd/^{144}Nd$.

4.3. Geochronology

Two samples representing early and late stages of the Conchagua Volcano evolution were selected for dating. An amphibole separate from the La Unión pumice (SG26A) yielded two results, 12.5 ± 3.7 and 14.2 ± 4.7 Ma (Tab. 2). Obviously, these values should be treated with caution due to large error caused by both the low-K content of amphibole, resulting in low content of radiogenic Ar, and by contamination with the atmospheric argon. The younger result of 12.5 ± 3.7 Ma is probably more realistic, because of a less atmospheric argon contamination. Therefore, a weighted mean result of 13.3 ± 3.7 Ma is preferred. The age of the second sample obtained from a fresh bulk rock basalt SG27 collected near Playitas yielded 1.6 ± 0.6 Ma. The age determination leads us to rank this lava to the Pre-Conchagua stage.

5. Discussion

5.1. Chronology of the Conchagua volcanism

The K–Ar dating of the La Unión pumice at 13.4 ± 3.7 Ma (mean age of amphibole) is similar to feldspar K–Ar ages given by Hradecký (2006) for the Chalatenango Formation (16.9 ± 0.5 and 14.8 ± 0.5 Ma) in northwestern El Salvador. Also Jordan et al. (2007) have dated ignimbrites (Ar–Ar, sanidine and plagioclase) of southern Honduras and western Nicaragua between 13.4 and 16.9 Ma. Reynolds (1980) correlated the Chalatenango Formation in El Salvador with the San Agustin Las Minas Formation in western Guatemala; the rhyolitic

ignimbrites of the latter were dated to 11.6 ± 0.5 and 9.4 ± 0.4 Ma (K–Ar).

The presence of coarse-grained fall-out deposits of the La Unión unit indicates a near vent origin and therefore it may be assumed that the hypothetical La Unión Volcano could indeed be one of the volcanic centres of the Chalatenango Formation.

The exact age of the Playitas Ignimbrites remains unconstrained. They might be correlated with the older – Oligocene – Morazán Formation or with similar ignimbrites of the younger – Miocene – Chalatenango Formation. A very general stratigraphic division by Wiesemann (1975) allows long time periods for each of the formations, where complex magmatic processes could have occurred producing distinct volcanic rocks. Worth noting is that Wiesemann (1975) has reported both silicic and mafic volcanic rocks from the Chalatenango Formation.

Explosivity of the evolved dacitic magma of the La Unión unit was probably increased by an influx of primitive basaltic melt and magma mixing as suggested by bimodal, banded pumice. In general, basaltic magma influx is thought to have a potential to trigger silicic volcanic eruptions (e.g., Sparks et al. 1977; Leonard et al. 2002; Hammer and Rutherford 2003). Fine-grained deposits produced by intense fragmentation at the base of each of the studied units represent a phreato-magmatic pulse initiating each period of eruptive activity. Phreatomagmatic phases commencing magmatic eruptions are described to have originated from both monogenic volcanoes (Schmincke 1977) and large composite volcanoes (e.g., Cioni 2000; Arce et al. 2003).

No outcrop with clear contact between the Playitas Ignimbrites and the Pozo unit was observed. However, a close link is inferred between the Pozo unit and the Bálsamo Formation and hence an age close to the Miocene–Pliocene boundary. The volcanic rocks of the Pozo unit are unfortunately too altered to be chemically analysed or dated.

Remnants of pines found in the El Naranjo maar near the shoreline (Hradecký 2003) imply that this eruption took place during a cooler period in the Pleistocene, probably synchronously to the Pre-Conchagua – Juana-Pancha volcanic activity.

The structure of the ill-sorted breccia at the base of the Ocotal succession and the presence of planar cross-bedded tuff (possibly surge deposit) suggest a pyroclastic flow sedimentation of this deposit. On the other hand, massive and poorly vesiculated volcanic fragments do not argue for pyroclastic origin. Massive angular fragments might have been produced by phreato-magmatic eruption of volatile-poor magma. The phreatomagmatic eruption fragmenting coherent volcanic rocks and volatile-poor magma could be related to an opening of the volcanic conduit, because the subsequent activity was much calmer and larger eruptions have not occurred ever since.

The Ar–Ar ages are younger for Ocotal (0.15 ± 0.02 Ma) than for Banderas (0.41 ± 0.1 Ma) cones (Quezada and García 2008). In contrary to the radiometric ages, the Banderas cone has a better preserved morphology, less affected by erosion and post-volcanic tectonics. Furthermore, the Banderas pyroclastic deposits partly overlay rock sequences of the Ocotal cone. Hence the contemporaneity of both cones, or relatively short time-span between them, may be suggested. No layers of fossil soils or fossil weathering interrupting volcanic sequences of both cones were observed. This is most probably due to relatively fast growth of the two. On the other hand, both cones are mantled by significant soil cover, suggesting that the volcano is extinct.

The source of the fine White ash filling the depressions in tectonic valleys could not be found in close surroundings. No silica-rich magma erupted on the Conchagua Peninsula since the La Unión unit (Miocene) which in any case produced dacitic (and not rhyolitic) tephra. The nearby Nicaraguan Cosigüina Volcano is dominantly andesitic with SiO_2 contents never exceeding 66 wt. % (Hradecký and Rapprich 2008) and the also close, even though somewhat more distant (50 km), Salvadorian San Miguel Volcano is basaltic (e.g., Chesner et al. 2004).

On the other hand, a violent eruption of the Ilopango Caldera (130 km to the west) took place in 430 AD (Dull et al. 2001) and deposits of this eruption (Tierra Blanca Joven) were recognised on many places all over Central America (e.g., Mehringer et al. 2005). Rhyolitic composition and absence of glass alteration suggest a young age for the White ash around Conchagua and support its correlation with distal Tierra Blanca Joven ashes.

5.2. Tectonics

Major faults and fractures were located on the basis of geological mapping and DEM analyses. There are three principal fault patterns observed in the wider surroundings of the Conchagua Volcano (Fig. 9). Faults trending WNW–ESE are parallel to the Salvadorian Graben (*syn.* Salvadorian Depression). Faults trending NNW–SSE are much more frequent, and occur mainly in the Olomega Lake area. The NNW–SSE oriented faults cut rocks of the Bálsamo Formation (*sensu* Wiesemann 1975) or Pozo unit and Pilón Lavas. The general trend of lineaments west of the studied area is NNW–SSE. Closer to the Conchagua Volcano to the east, where younger volcanic rocks dominate, the general trend of lineaments shifts to NNE–SSW. The latter faults appear to form horst and graben structures and hence it is supposed that they are mostly of normal character. The NNE trending pattern of fractures around the Concha-

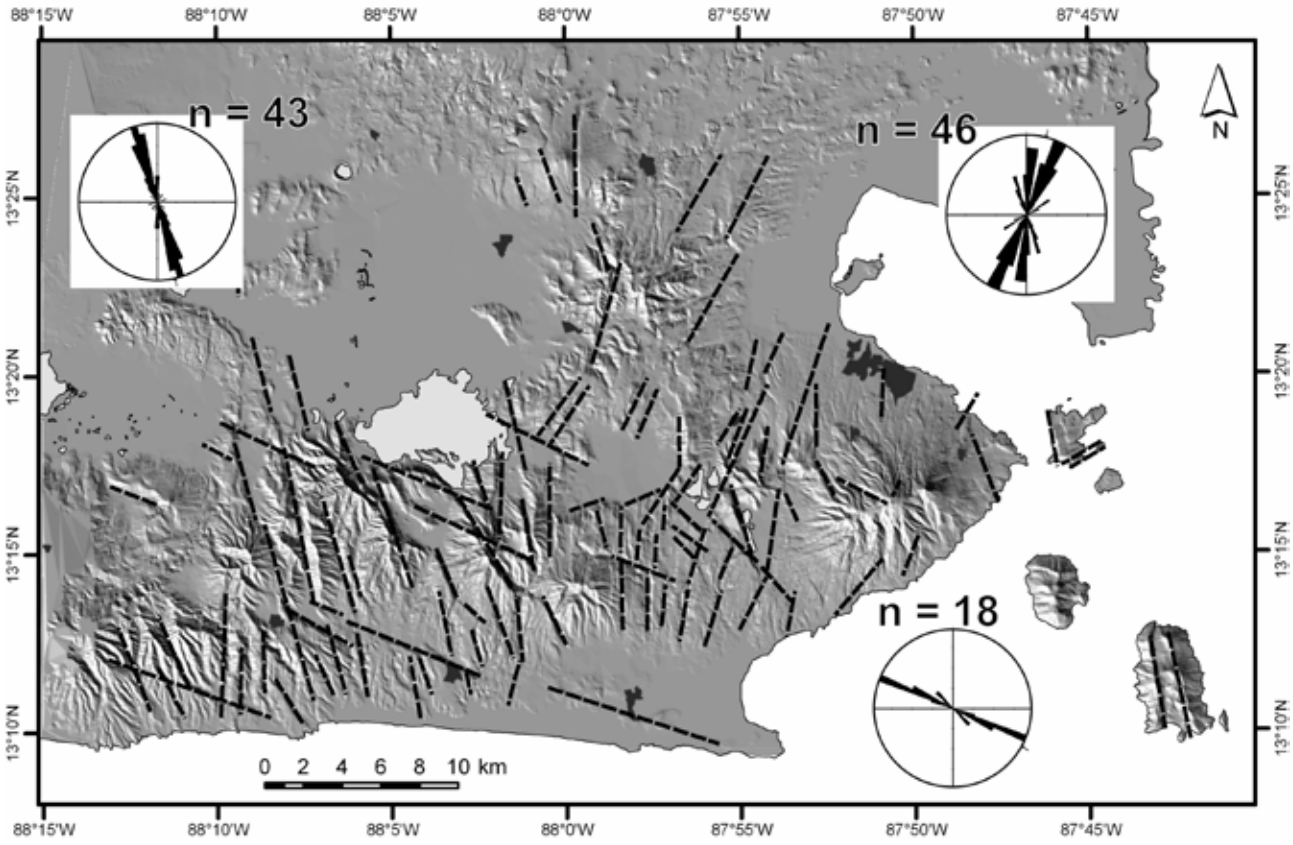

Fig. 9 Digital elevation model (DEM) image showing principal lineaments in wider surroundings of the Conchagua Volcano. Inset rose diagrams display preferred orientation of faults and fractures in the Olomega Lake area (west of 88° W – top left), close vicinity of the Conchagua Volcano (east of 88° W – top right) and faults related to the Salvadorian Graben (*syn.* Salvadorian Depression, crosses both previous areas – bottom right).

gua Volcano corresponds to the southern segment of the Comayagua Graben in Honduras. Given the geographic position of both areas and trend of the faults (Fig. 9), it is suggested that the Conchagua area represents the southern edge of the Comayagua Graben. The general fault trend changes clockwise from NNW–SSE, cutting the rocks of probably Pliocene age, to NNE–SSW faults that affect also rocks as young as Pleistocene. Assuming a generally stable orientation of the regional stress field, such a fan-like arrangement could be explained by anticlockwise rotation of the Chortis Block (Gordon and Muehlberger 1994), except for the part east of the Guayape Fault, affected by dextral movements on the same fault.

The NE–SW to ENE–WSW trending faults comparable with orientation of the Guayape Fault Zone were documented only at the southern margin of the Zacatillo Island. The Guayape Fault Zone probably played an important role in the formation of the Gulf of Fonseca and represents a boundary between crustal blocks and volcanic arc segments. However, it most probably did not directly influence the evolution of the Conchagua Peninsula.

5.3. Geochemistry

In general, basic and intermediate lavas share the main features with other volcanic front volcanoes in the region, i.e. low HFSE contents and elevated LILE (cf. database of Carr et al. 2003). This clearly mirrors the process of melting of the depleted mantle wedge by influx of slab-derived fluid or melt. This process was in detail described from volcanic arcs worldwide, including CAVA (see Carr et al. 2007 for review). Indeed, in the Ti–V diagram (Shervais 1992) the samples SG27 and SG26A, together with published Conchagua data, fall within the field of high oxygen fugacity typical of arc lavas (ARC in Fig. 8c). However, two samples, both members of the Pre-Conchagua – Juana-Pancha lithostratigraphic unit, show slightly different geochemical fingerprint.

As documented in the geochemistry section, samples SG27 and S03/139B have low Ba/Nb and Ba/La ratios taken as indicating the presence of sediment-derived subduction fluid (Carr et al. 2003; Pearce and Stern 2006). This suggests limited involvement of such a fluid in generation of these lavas. On the other hand, the

same two samples show low Zr/Nb ratios (8.3 and 10.2) whereas the others reach values exceeding 20, comparable to volcanic front lavas (Carr et al. 2003). Low Zr/Nb ratios (e.g. below ~ 20) suggest a less depleted parental mantle source of SG27 and S03/139B. Sample SG27 has also very low Th/Nb (0.15). For subduction-related magmas this ratio is typically higher (up to 1.6, only seldom below 0.2), indicating an involvement of supercritical melt derived from deeply subducted slab (Elliott 2003).

Such low Th/Nb and Zr/Nb values resemble those for lavas from the Tegucigalpa (Th/Nb ~ 0.1–0.5, Zr/Nb ~ 7–30) and Yojoa (Th/Nb bellow 0.1, Zr/Nb ~ 4.5–9) volcanic fields in Honduras, situated behind the main volcanic front (BVF, Walker et al. 2000; Carr et al. 2003), where BVF lavas show only limited, if any, influx of fluid/melt-mobile elements from subducted slab. The Tegucigalpa and Yojoa lavas were interpreted as products of decompression-driven partial melting of undepleted continental mantle, with minor role for the subduction-related fluid/melt (Walker et al. 2000).

As evidenced by the geological map of Rogers (2003), the Comayagua Graben connects the Tegucigalpa volcanic field with the Gulf of Fonseca area. This graben is also a major tectonic divide separating two segments of the CAVA (Stoiber and Carr 1973). On this boundary, significant right-lateral offset of the two segments occurs, and also a major change in the slab top depth under the volcano: 146 km beneath Conchagua, and 116 km beneath Cosigüina southeast of the Gulf of Fonseca (Syracuse and Abers 2006). Furthermore, Bolge (2005) observed an abrupt change in some HFSE indicators at this boundary, with the Zr/Nb ratios changing from ~30 to ~60 towards the east. These values are in good agreement with most of our data, but still too high to explain the low Zr/Nb ratios of samples SG27 and S03/139B. Therefore, the origin of some lavas of the Pre-Conchagua – Juana-Pancha lithostratigraphic unit was likely controlled by interplay of tectonic processes at the orthogonal intersection of the volcanic front and the Comayagua Graben. This includes combination of melting of depleted mantle triggered by fluid/melt influx from the subducting Cocos plate, extension-driven decompression melting of a less depleted mantle source at the Comayagua Graben (similarly to the Tegucigalpa area) or even influx of less depleted melts from areas behind the volcanic front.

Taken together, such a model implies extension in the Comayagua Graben during early Pleistocene. Since we are not aware of any available geochronological data from the Tegucigalpa volcanic field, it is not possible to compare the age of this volcanic activity with the Pre-Conchagua – Juana-Pancha unit.

6. Conclusions

Detailed geological mapping of the Conchagua Peninsula resulted in postulation of several new lithostratigraphic units. The La Unión unit is of Miocene age and correlates with the Chalatenango Formation. Dacitic eruptions were the most probably triggered by mafic injection(s) as indicated by bimodal composition of pyroclastic rocks. Since mid-Miocene, no silicic magmas erupted on the Conchagua Peninsula. Pre-Conchagua basaltic andesites and Ocotal and Banderas basaltic cones build the main edifice of the Conchagua Volcano. The latter two consist of Strombolian scoriae deposits intercalated with olivine basalt lavas. Significant soil cover has evolved on both cones suggesting that the volcano is extinct. The youngest White ash unit found in the lowland area most probably represents distal facies of the Tierra Blanca Joven fall-out.

Morphology of the Conchagua Peninsula is influenced by three tectonic systems. Comayagua Graben-related faults are associated with small local grabens containing Holocene sedimentary and volcanic infill. Anticlockwise rotation of the Chortis Block could be traced in change of tectonic lineaments orientation (clockwise rotated in younger rocks if compared to the older ones).

Majority of the sampled rocks carry the subduction imprint, similarly to adjacent CAVA volcanoes. Two samples of the Pre-Conchagua unit have lower Zr/Nb, Th/Nb, Ba/La and Ba/Nb ratios suggesting involvement of a melt from a distinct magma source. These samples differ in their trace-element composition from the common Volcanic Front lavas and instead resemble those of the Tegucigalpa volcanic field. This could be explained by the influx of the decompression melt associated with extension in the Comayagua Graben.

Acknowledgements. Research on the Conchagua Volcano was supported by the project 205/06/1811 of the Czech Science Foundation (GAČR, to VE) and by the Research Plan of the Czech Geological Survey (MZP0002579801). The Czech Ministry of Foreign Affairs supported the first field campaign in 2003 within the framework of development cooperation project. Thanks are due to Rod Holcombe, whose GEOrient software was provided free of charge for scientific use. Special thanks are given to members of the first (2003) field campaign Petr Hradecký, Pavel Havlíček, Štěpánka Mrázová, Jiří Šebesta and Tomáš Vorel (all Czech Geological Survey, Prague), Josef Ševčík (Gekon Ltd., Prague) and Carlos Pullinger (SNET, currently LaGeo, San Salvador). We also would like to thank to Brian Hausback, Ioan Seghedi, Jaroslav Lexa and an anonymous reviewer for their constructive comments as well as Miroslav Štemprok for careful editorial handling.

Electronic supplementary material. Morphometric analysis of the Conchagua Peninsula. Landscape geometry has been calculated and visualized according to morphostructures and slope dip is available online at the Journal web site (http://dx.doi.org/10.3190/jgeosci.069).

References

Arce JL, Macías JL, Vázquez–Selem L (2003) The 10.5 ka Plinian eruption of Nevado de Toluca volcano, Mexico: stratigraphy and hazard implications. Geol Soc Am Bull 115: 230–248

Bellon H, Quoc Buü N, Chaumont J, Philippet JC (1981) Implantation ionique d'argon dans une cible support: application au traçage isotopique de l'argon contenu dans les minéraux et les roches. C R Acad Sci Paris 292: 977–980

Bolge LL (2005) Constraining the Magmatic Sources of Hawaiian and Central American Volcanics. Unpublished Ph.D. thesis, The State University of New Jersey, New Brunswick, pp 1–281

Bolge LL, Carr MJ, Milidakis KI, Lindsay FN, Feigenson MD (2009) Correlating geochemistry, tectonics, and volcanic volume along the Central American volcanic front. Geochem Geophys Geosyst 10: doi 10.1029/2009GC002704

Burkart B, Self S (1985) Extension and rotation of crustal blocks in northern Central America and effect on the volcanic arc. Geology 13: 22–26

Carr MJ (1984) Symmetrical and segmented variation of physical and geochemical characteristics of the Central American volcanic front. J Volcanol Geotherm Res 20: 231–252

Carr MJ, Mayfield DG, Walker JA (1981) Relation of lava compositions to volcano size and structure in El-Salvador. J Volcanol Geotherm Res 10: 35–48

Carr MJ, Feigenson MD, Patino LC, Walker JA (2003) Volcanism and geochemistry in Central America; progress and problems. In: Eiler JM (ed.) Inside the Subduction Factory. American Geophysical Union, Geophysical Monograph 138: 153–174

Carr MJ, Patino LC, Feigenson MD (2007) Petrology and geochemistry of lavas. In: Bundschuh J, Alvarado GE (eds) Central America: Geology, Resources and Hazards. Taylor & Francis, London, pp 565–590

Chesner CA, Pullinger CR, Escobar CD (2004) Physical and chemical evolution of San Miguel Volcano, El Salvador. In: Rose WI, Bommer JJ, Lopez DL, Carr MJ, Major JJ (eds) Natural Hazards in El Salvador. Geological Society of America Special Papers 375: 213–226

Cioni R (2000) Volatile content and degassing processes in the AD 79 magma chamber at Vesuvius (Italy). Contrib Mineral Petrol 140: 40–54

Corti G, Carminati E, Mazzarini F, Garcia MO (2005) Active strike-slip faulting in El Salvador, Central America. Geology 33: 989–992

Dull RA, Southon JR, Sheets P (2001) Volcanism, ecology and culture: a reassessment of the Volcan Ilopango TBJ eruption in the Southern Maya Realm. Latin Amer Antiq 12: 25–44

Elliott T (2003) Tracers of the slab. In: Eiler JM (ed.), Inside the Subduction Factory. American Geophysical Union, Geophysical Monograph 138: 23–45

Finch RC, Ritchie AW (1991) The Guayape fault system, Honduras, Central America. J South Amer Earth Sci 4: 43–60

Funk J, Mann P, McIntosh K, Stephens J (2009) Cenozoic tectonics of the Nicaraguan depression, Nicaragua, and Median Trough, El Salvador, based on seismic-reflection profiling and remote-sensing data. Geol Soc Am Bull 121: 1491–1521

Global Volcanism Program (2009) Conchagua, *http://www.volcano.si.edu/world/volcano.cfm?vnum=1403-11=*. Visited on June 2nd, 2009

Gordon MB, Muehlberger WR (1994) Rotation of the Chortis Block causes dextral slip on the Guayape Fault. Tectonics 13: 858–872

Hammer JE, Rutherford MJ (2003) Petrologic indicators of preeruption magma dynamics. Geology 31: 79–82

Holcombe R GEOrient v9.x. *http://www.holcombe.net.au/software/rodh_software_georient.htm*. Visited on June 2nd, 2009

Hradecký P (2006) Tertiary ignimbrites in Central America: volcanological aspects and lithostratigraphical proposal. Krystalinikum 31: 11–24

Hradecký P, Rapprich V (2008) Historical tephra-stratigraphy of the Cosigüina Volcano (Western Nicaragua). Rev Geol Amér Central 38: 65–79

Hradecký P, Havlíček P, Mrázová Š, Rapprich V, Šebesta J, Ševčík J, Vorel T, Pullinger C, Hernández W (2003) Geological study of natural hazards in the region of La Unión and the Gulf of Fonseca, El Salvador/Estudio de los peligros geológicos en el departamento de La Unión y de Golfo Fonseca, El Salvador. Unpublished Final Report, Czech Geological Survey, Prague, Servicio Nacional de Estudios Territoriales, San Salvador, pp 1–96 (in Czech and Spanish)

Janoušek V, Farrow CM, Erban V (2006) Interpretation of whole-rock geochemical data in igneous geochemistry: introducing Geochemical Data Toolkit (GCDkit). J Petrol 47: 1255–1259

Jordan BR, Sigurdsson H, Carey S, Lundin S, Rogers RD, Singer B, Barquero–Molina M (2007) Petrogenesis of Central American Tertiary ignimbrites and associated Caribbean Sea tephra. In: Mann P (ed.) Geologic and Tectonic Development of the Caribbean Plate Boundary in Northern Central America. Geological Society of America Special Papers 428: 151–179

Le Bas MJ, Le Maitre RW, Streckeisen A, Zanettin B (1986) A chemical classification of volcanic rocks based on the total alkali-silica diagram. J Petrol 27: 745–750

Leonard GS, Cole JW, Nairn IA, Self S (2002) Basalt triggering of the c. AD 1305 Kahaora rhyolite eruption, Tarawera Volcanic Complex, New Zealand. J Volcanol Geotherm Res 115: 461–486

Mahood G, Drake RE (1982) K–Ar dating young rhyolite rocks: a case study of the Sierra La Primavera, Jalisco, Mexico. Geol Soc Am Bull 93: 1232–1241

Mehringer Jr PJ, Sarna–Wojcicki AM, Wollwage LK, Sheets P (2005) Age and extent of the Ilopango TBJ Tephra inferred from a Holocene chronostratigraphic reference section, Lago De Yojoa, Honduras. Quater Res 63: 199–205

Meyer-Abich H (1956) Los volcánes activos de Guatemala y El Salvador. Anales del Servicio Geologico Nacional de El Salvador, San Salvador, pp 1–102

Míková J, Denková P (2007) Modified chromatographic separation scheme for Sr and Nd isotope analysis in geological silicate samples. J Geosci 52: 221–226

Miyashiro A (1974) Volcanic rock series in island arcs and active continental margins. Amer J Sci 274: 321–355.

Pearce JA (1996) A user's guide to basalt discrimination diagrams. In: Wyman DA (ed.) Trace Element Geochemistry of Volcanic Rocks: Applications for Massive Sulphide Exploration. Geological Association of Canada, Short Course Notes 12: pp 79–113

Pearce JA, Stern RJ (2006) Origin of back-arc basin magmas: trace element and isotope perspectives. In: Christie DM, Fisher CR, Lee S-M, Givens S (eds), Back-Arc Spreading Systems: Geological, Biological, Chemical, and Physical Interactions. American Geophysical Union, Geophysical Monograph 166: 63–86

Phipps–Morgan J, Ranero CR, Vannucchi P (2008) Intra-arc extension in Central America: links between plate motions, tectonics, volcanism, and geochemistry. Earth Planet Sci Lett 272: 365–371

Quezada AM, García OM (2008) Edades $^{40}Ar/^{39}Ar$ de rocas de las áreas de Conchagua y Chilanguera (El Salvador). Unpublished Report, LaGeo, Santa Tecla, pp 1–19

Reynolds JH (1980) Late Tertiary volcanic stratigraphy of northern Central America. Bull Volcanol 43: 601–607

Rogers RD (2003) Jurassic–Recent tectonic and stratigraphic history of the Chortis Block of Honduras and Nicaragua (northern Central America). Unpublished Ph.D. thesis, University of Texas, Austin, pp 1–289

Sapper K (1925) The Volcanoes of Central America. Verlag Max Niemeyer, Halle, pp 1–144

Schmincke H-U (1977) Phreatomagmatische Phasen in quartären Vulkanen der Osteifel. Geol Jb 39: 3–45

Shervais JW (1992) Ti–V plots and the petrogenesis of modern and ophiolitic lavas. Earth Planet Sci Lett 59: 101–118

Silva–Romo G (2008) Guayape–Papalutla fault system: a continuous Cretaceous structure from southern Mexico to the Chortis Block? Tectonic implications. Geology 36: 75–78

Sparks RSJ, Sigurdsson H, Wilson L (1977) Magma mixing; a mechanism for triggering acid explosive eruptions. Nature 267: 315–318

Steiger RH, Jäger E (1977) Subcommission on Geochronology: convention on the use of decay constants in geo- and cosmochronology. Earth Planet Sci Lett 36: 359–362

Stoiber RE, Carr MJ (1973) Quaternary volcanic and tectonic segmentation of Central America. Bull Volcanol 37: 304–325.

Syracuse EM, Abers GA (2006) Global compilation of variations in slab depth beneath arc volcanoes and implications. Geochem Geophys Geosyst 7: doi:10.1029/2005GC001045

Tonarini S, Agostini S, Doglioni C, Innocenti F, Manetti P (2007) Evidence for serpentinite fluid in convergent margin systems: the example of El Salvador (Central America) arc lavas. Geochem Geophys Geosyst 8: doi:10.1029/2006GC001508

Walker JA, Patino LC, Cameron BI, Carr MJ (2000) Petrogenetic insights provided by compositional transects across the Central American arc: southeastern Guatemala and Honduras. J Geophys Res 105: 18949–18963

Weber HS, Wiesemann G (1978) Mapa Geologico de la República de El Salvador/America Central. Bundesanstalt für Geowissenschaften und Rohstoffe, Hannover. Geological map on 1:100 000 scale in 6 sheets

Weber HS, Wiesemann G, Wittekindt H (1974) Mapa geológico General de la República de El Salvador 1:500 000. Bundesanstalt für Bodenforschung, Hannover

Weyl R (1980) Geology of Central America. Borntraeger, Berlin, pp 1–371

Wiesemann G (1975) Remarks on the geologic structure of the Republic of El Salvador, Central America. Mitt Geol Paläont Inst Univ Hamburg 44: 557–574

Wood JD (1996) The Geomorphologic Characterization of Digital Elevation Models. Unpublished Ph.D. thesis, University of Leicester, Leicester. *http://www.soi.city.ac.uk/~jwo/phd*. Visited June 4th, 2009